**Joseph M. Kahn**
**September 4, 2008**

**Simulation of Polarization-Multiplexed Orthogonal Frequency-Division Multiplexing using QPSK**

## *1. Introduction*

In principle, ignoring nonlinear effects, using coherent detection, the performance of single-carrier modulation is identical to that of multi-carrier modulation [1]. Moreover, when the two types of systems are implemented well, their implementation complexity is similar [1]. In practice, the two types of systems do differ significantly in many implementation details, and the two types of systems are subject to different degrees of impairment by various effects, especially fiber nonlinearity. To date, most studies have addressed one or the other type of system, and few, if any, studies have attempted to make a fair comparison.

In this report, I describe the modeling and simulation of a system using polarization-multiplexed (PM) orthogonal frequency-division multiplexing (OFDM) with QPSK modulation and digital coherent detection. I have written MATLAB code to simulate an OFDM transmitter, propagation through optical fiber, and a coherent OFDM receiver. This code has been used to study the performance of an OFDM system and to test its sensitivity to several key design parameters in the transmitter and receiver. As in my previous studies of PM single-carrier QPSK, due to time and software constraints, I have only simulated linear propagation of a single wavelength. I expect that Christian Malouin will adapt my code to his MATLAB simulation environment and use it to perform studies comparing OFDM to single-carrier QPSK in a nonlinear WDM system environment. Alternately, if Christian prefers, I would be willing to use his nonlinear propagation code to perform such simulations myself.

I should note that some of my graduate students at Stanford are actively working on research comparing the nonlinear tolerance of OFDM and single-carrier QPSK. Their results to date have shown that in long-haul systems using conventional inline optical chromatic dispersion (CD) compensation, the optimal launched power for OFDM is roughly 2 dB lower than for single-carrier, so that the reach of OFDM is significantly less than that of single-carrier. They are completing these studies, by considering systems not using inline CD compensation and by considering simple signal processing methods to compensate fiber nonlinearity. I anticipate that this work will be documented in a paper within the next few weeks, which I will be happy to share with StrataLight. In view of the need to prevent a conflict of interest, I am not able to use their code, nor share it with StrataLight (in any case, their code is not sufficiently portable or well-documented to be transferred to StrataLight).

## *2. Design of OFDM System*

The OFDM transmitter and receiver are shown in Fig. 1. Detailed explanations of their design and optimization are given in [2] and [3]. Key design issues are described briefly here.

In the OFDM transmitter, in each polarization, data are modulated onto blocks of $N_u$ QPSK symbols. The parameter $N_u$ is the number of used subcarriers (in our system design example, $N_u = 52$). In order to compensate for the effect of the transmitter lowpass filter (i.e., the response of the analog output of the D/A converter), each QPSK symbol in a block is multiplied by the inverse of the frequency response of the lowpass filter at the respective subcarrier frequency. Next, $N_c - N_u$ zero symbols are inserted into each block of $N_u$ QPSK symbols, extending the block length to $N_c$. The parameter $N_c$ is the total number of carriers, and is equal to the IDFT and DFT block lengths. Usually, $N_c$ is chosen to be an integer power of 2, in order to maximize IDFT/DFT efficiency. In OFDM, these zero symbols or zero subcarriers are inserted in order to implement oversampling at the transmitter and receiver by a ratio is $N_c/N_u$ (in our example $N_c/N_u \approx 1.23$). A key advantage of OFDM is that it enables arbitrary rational oversampling ratios, as opposed to single- carrier modulation, where only integer or half-integer oversampling ratios

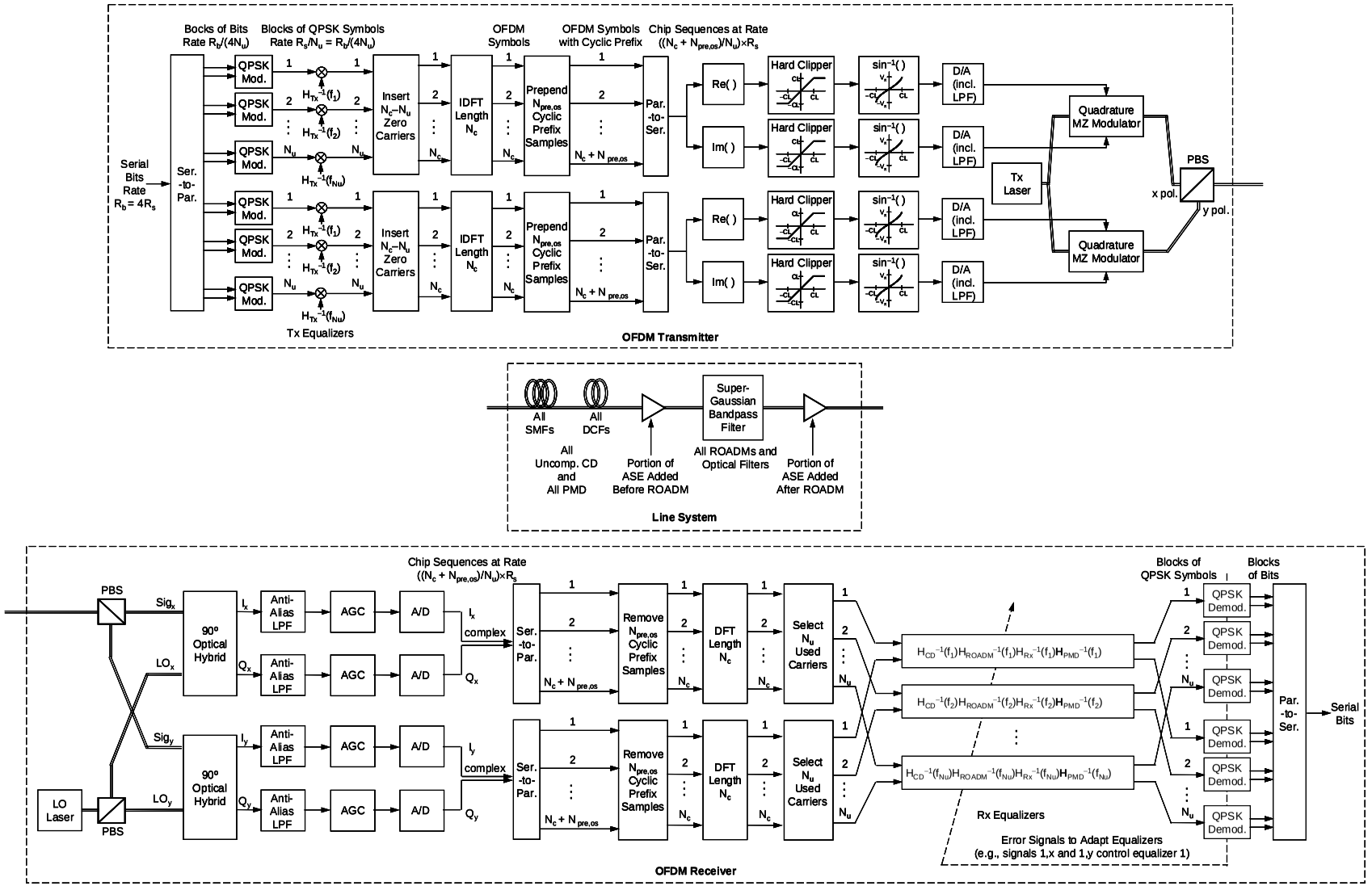


**Fig. 1.** Design of transmitter and receiver for polarization-multiplexed OFDM using QPSK. Also shown is the transmission line system as modeled in our simulations.

are practical. Once the zero symbols are inserted, the IDFT of each block of $N_c$ symbols is taken. This operation serves to modulate the $N_u$ QPSK symbols onto $N_u$ subcarriers, which are at positive and negative frequencies near baseband.

In order to mitigate intersymbol interference (ISI) that may originate from fiber dispersion or from electrical filters, the OFDM transmitter takes some of the samples from the end of each OFDM symbol block and prepends them to the start of the block. This prepended set of samples is called the cyclic prefix. The parameter $N_{pre}$ is the nominal cyclic prefix length. Accounting for oversampling, the actual cyclic prefix length becomes $N_{pre,os} = \lceil (N_c / N_u) N_{pre} \rceil$, where $\lceil \ \rceil$ is the ceiling function. We must choose $N_{pre,os}$ so that the cyclic prefix duration is at least equal to the delay spread of the channel (as explained in [1],[2], when the delay spread is infinite, as in the case of CD, the cyclic prefix length should be chosen to span almost all of the energy in the impulse response). With the $N_{pre,os}$ cyclic prefix samples prepended, the length of each block is extended to $N_c + N_{pre,os}$. Hence, adding the cyclic prefix induces a sampling rate penalty and an optical power penalty, increasing both by the ratio $(N_c + N_{pre,os})/N_c$. In order to reduce the cyclic prefix penalty to a suitably small value, we must increase the number of used subcarriers $N_u$, thus increasing $N_c$. Unfortunately, increasing the number of subcarriers decreases tolerance to laser phase noise, decreases optical modulator efficiency [3], and exacerbates nonlinear effects in fiber propagation [4].

ISI mitigation by the cyclic prefix can be explained as follows. Passing a signal through the fiber and electrical filters corresponds to *linear convolution* with an impulse response. When an OFDM symbol block with cyclic prefix is linearly convolved with this impulse response, then a suitably chosen block of $N_c$ samples corresponds to a *circular convolution* between the OFDM symbol block (without cyclic prefix) and this impulse response. The OFDM receiver takes the $N_c$-point DFT of the block of $N_c$ samples, yielding a block of $N_c$ modulated subcarriers. Since the time-domain block was subject to a circular convolution, its DFT, the frequency-domain block, has each element multiplied by a complex number, which corresponds to the frequency response of the fiber and filters at the respective subcarrier frequency. Provided the cyclic prefix is sufficiently long, the subcarriers remain orthogonal, i.e., there is no ISI. Distortion caused by the fiber and filters can be undone simply by multiplying each subcarrier by the inverse of the fiber/filter frequency response.

Returning to the OFDM transmitter in Fig. 1, once the cyclic prefix samples are prepended, we must perform some additional DSP to increase transmitter optical power efficiency and compensate for the sinusoidal transfer characteristic of the Mach-Zehnder modulators, as described in [3]. For a typical number of subcarriers, an OFDM waveform has a high peak-to-average amplitude ratio, but the peaks come very infrequently. We can perform hard clipping of the waveform to remove the peaks, while introducing acceptably small degradation. Each hard clipper has clipping level $CL$, restricting the signal to the range $\pm CL$. We then perform the $\sin^{-1}()$ operation to precompensate for the modulator transfer characteristic, mapping the range $\pm CL$ to the range $\pm V_\pi$. The precompensated samples are fed to the D/A converters, in order to interpolate the samples to form modulator drive waveforms. The D/A converter inputs are quantized to a finite number of bits. The D/A converter interpolation is defined by its output stage, which is assumed to have a Butterworth filter frequency response.

At the OFDM receiver in Fig. 1, the received signal and local oscillator are combined in two orthogonal polarizations, and downconverted to yield inphase and quadrature (I and Q) baseband components. To minimize aliasing, these are filtered by Butterworth lowpass filters, and are scaled by an automatic gain control. These signals are sampled once per OFDM sample and are quantized to finite bit precision by A/D converters. Cyclic prefix samples are removed, $N_c$-point DFTs are performed to demodulate the OFDM symbols, and the amplitudes of the $N_u$ used subcarriers are selected. A bank of receiver equalizers compensates for the effects of CD, PMD, optical filtering, and receiver electrical filtering, multiplying by the inverse of the overall frequency response at the respective subcarrier

frequencies. At the $i$th subcarrier frequency $f_i$, PMD intermixes the signals in the two orthogonal polarizations, which can be described as multiplying a 2 × 1 column vector by the 2 × 2 Jones matrix $\boldsymbol{H}_{PMD}(f_i)$ at the $i$th subcarrier frequency. This is undone by multiplying the received 2 × 1 column vector by the inverse Jones matrix $\boldsymbol{H}^{-1}{}_{PMD}(f_i)$.

In simulation, where all frequency responses are known, the receiver equalizers can be computed precisely. In practice, the receiver equalizers are adapted using a common algorithm, such as LMS. We have considered both ideal and adaptive equalizers in our simulations.

### *3. MATLAB Simulation Code*

#### *a. Design of Code*

The MATLAB code comprises a main routine **`ofdm_twopol_adaptive.m`**, which uses the functions **`quantz.m`** and **`spectrum_periodogram.m`**, along with several MATLAB toolbox functions, **`randint.m`**, **`qammod.m`**, **`qamdemod.m`**, and **`symerr.m`**. The code is extensively documented.

We note that in the OFDM system being modeled, the effective oversampling rate is $M_s = N_c/N_u$, which equals the rate at which digital samples are generated and processed, divided by the rate at which information-bearing QPSK samples are encoded and decoded. In our simulation, we introduce an additional oversampling rate $M_{ct}$, which is the sampling rate at which continuous-time waveforms are emulated, divided by the rate at which digital samples are generated and processed. When we choose $M_s = N_c/N_u \approx 1.23$, there is minimal aliasing, and our simulation yields almost the same results for any value of $M_{ct}$, all the way down to $M_{ct} = 1$. All of the simulations presented here were performed at $M_{ct} = 2$. In the presence of nonlinear fiber effects, I expect it will be necessary to increase $M_{ct}$ to a higher value.

To model long-haul transmission, the code includes lumped optical amplification, CD, all-order PMD, and tight optical filtering by (de)multiplexers and ROADMs. For simplicity, all optical filters are lumped into one variable-order super-Gaussian filter, with some fraction of the ASE added before the filter, and the remainder of the ASE added after the filter.

#### *b. Simulation Example*

The main routine **`ofdm_twopol_adaptive.m`** begins with a list of all the system and simulation parameters to set. In this simulation example, the parameters were set as follows.

```
% Modulation parameters
Nu = 52;                % number of used subcarriers (must be even)
Nc = 64;                % total number of subcarriers = FFT size (must be even)
Npre = 10;              % total cyclic prefix length (ref. to 1 sample/chip)
Ms = Nc/Nu;             % oversampling ratio
CS = 4;                 % constellation size (4 corresponds to QPSK)
Rb = 112e9;             % bit rate (total over two polarizations) (b/s)
Rs = Rb/(2*log2(CS));   % symbol rate (Hz)

% Transmitter parameters (for values chosen, Butterworth filter, not interpolator, is
% bandwidth-limiting element)
clip_level = 0.60;          % clipping level (V) (should adjust to get best results)
Vpi = 5;                    % switching voltage of modulator
txquantrange = 2*Vpi;       % range between max and min levels of Tx D/A (V) (should be 2*Vpi when
clipping level set properly)
txquantbits = 8;            % bits of quantization of Tx D/A
interp_length = 9;          % length parameter for interpolator at Tx
interp_cutoff = 0.8;        % cutoff parameter for interpolator at Tx
tx_but_ord = 5;             % order of Butterworth filter at Tx
tx_but_cutoff_norm = 0.5;   % cutoff frequency of Butterworth filter Tx (normalized to chip rate)
lambdanm = 1550;            % Wavelength (nm)
```

```
PlaserdBm = 6;              % power of CW laser
PtxdBm_ber = [-9:1.5:0];    % transmit signal powers at which to measure BER
PtxdBm_adapt = -3;          % power at which to do adaptation
PtxdBm_display = -3;        % power at which to display received spectrum, scatter plots of signal
                            % constellations, etc.
PtxdBm_scan = [PtxdBm_adapt, PtxdBm_ber, PtxdBm_display];

% Receiver parameters
rx_but_ord = 5;             % order of Butterworth filter at Rx
rx_but_cutoff_norm = 1/2;   % cutoff frequency of Butterworth filter Rx (normalized to chip rate)
rxagcrms = 0.15;            % filtered signal is scaled to this rms voltage before sampling and
quantization
rxquantrange = 0.75;        % range between max and min levels of Rx A/D (V)
rxquantbits = 8;            % bits of quantization of Rx A/D

% LMS algorithm
muinit = 0.005;             % initial value of step size parameter
mufactor = 0.1;             % a factor less than one
muinterval = 768;           % multiply mu by mufactor each time k increments by muinterval
mushifts = 1;               % Number of gear shifts. Stop multiplying mu by mufactor once k reaches
                            % muinterval*(mushifts+1)
startdd = 128;              % symbol at which to change from trained mode to decision-directed mode

% Loss and length
alphadBkm = 0.25;       % fiber loss (dBm/km)
Nspan = 25;             % number of fiber spans
Lspankm = 80;           % length per fiber span (km)
Lkm = Nspan*Lspankm;    % fiber length (km)

% Chromatic dispersion
Dpsnmkm = 17;           % CD (ps/(nm*km))
comppercent = 96;       % CD optical compensation (%)

% Polarization-mode dispersion
pmd = 'y';
taumeanps = 30;                 % mean DGD (ps)
Nsect = 10;                     % number of sections used to generate PMD
realiznumb = 1;                 % realization number
jmoldnew = 'old';               % if 'old': use existing Jones matrix jmfilename.mat
                                % if 'new': create and store new Jones matrix jmfilename.mat
                                % Note: must choose 'new' if change oversampling rate, number of carriers
                                % or cyclic prefix length.
% EDFA
NFdB = 5.0;                     % EDFA noise figure (dB)

% ROADM
ROADMord = 2;                   % ROADM super-Gaussian order
ROADMbw = 50e9;                 % ROADM bandwidth at -3 dB (Hz)
pre_ROADM_ASE_percent = 50;     % percent of ASE addded before ROADM (unitless, between 0 and 100)

% Simulation parameters
newsignal = 'n';                % 'y': generate new signal for each power level, 'n': generate one signal
for all power levels
newnoise = 'n';                 % 'n': generate new noise for each power level, 'n': generate one noise
for all power levels
Nsymb = 2^10;                   % number of OFDM symbols
Mct = 2;                        % oversampling rate for emulation of continuous time
fplotmax = 25e9;                % maximum frequency for plots of frequency-dependent quantities
osnrnoisebw = 50e9;             % optical filter bandwidth for measurement of optical signal-to-noise
ratio
```

```
Npdg = 8;                       % block length for periodogram
ch_sel = [1 Nu/2 Nu/2+1 Nu];    % channels selected to display scatter plot of signal constellation
smoothlength = 8;               % window length for smoooothing error plots
eqmagmindB = -20;               % min and max magnitudes and phases for plots of equalizer coefficients
eqmagmaxdB = 10;
eqphsmin = -1*pi;
eqphsmax = 5*pi;
```

Note the following key parameters:

| | |
|---|---|
| Bit rate | $R_b$ = 112 Gbit/s |
| Number of used subcarriers | $N_u$ = 52 |
| Number of subcarriers | $N_c$ = 64 |
| Cyclic prefix length | $N_{pre}$ = 10 |
| OFDM symbol duration | $T_{ofdm} = N_u/R_s = 4N_u/R_b$ = 1.857 ns |
| Transmission line system | 25 spans × 80 km of SMF with DCF and EDFAs |
| EDFA noise figure | 5.0 dB |
| Uncompensated CD | 1360 ps/nm |
| Mean DGD | 30 ps |
| Optical bandpass filter | 2nd order super-Gaussian |
| Optical filter bandwidth | 50 GHz |
| Transmitter and receiver quantization | 8 bits |

All received spectra, waveforms and constellation diagrams are recorded when the transmitted power is −3 dBm, corresponding to an OSNR of 10 dB (in 2 polarizations in 50-GHz bandwidth). The adaptive equalizer is also adapted at −3-dBm transmitted power, corresponding to 10-dB OSNR.

Fig. 2 describes the all-order PMD generated in the simulation example. The mean DGD is 30 ps. A concatenation of ten sections, each comprising a high-birefringence element and a random unitary transformation, were employed.

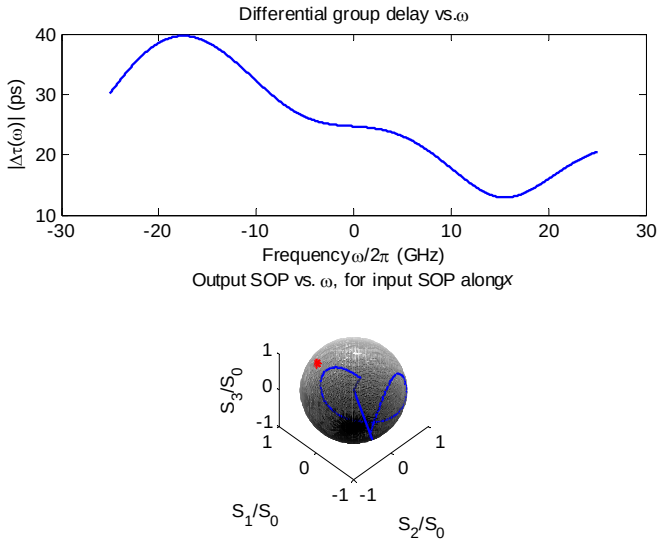


**Fig. 2.** Example of all-order PMD generated in simulation. The mean DGD is 30 ps. The upper graph shows magnitude of DGD vs. frequency. The lower graph shows the output SOP as a function of frequency, assuming the input SOP is along the *x* axis.

Fig. 3 shows power spectra of the transmitted and received OFDM signals. In the transmitted spectrum, all subcarriers have nearly equal amplitudes. In the received spectrum, edge carriers have been slightly attenuated by optical filtering, and a noise floor near −122 dBm/Hz is observed, originating from ASE.

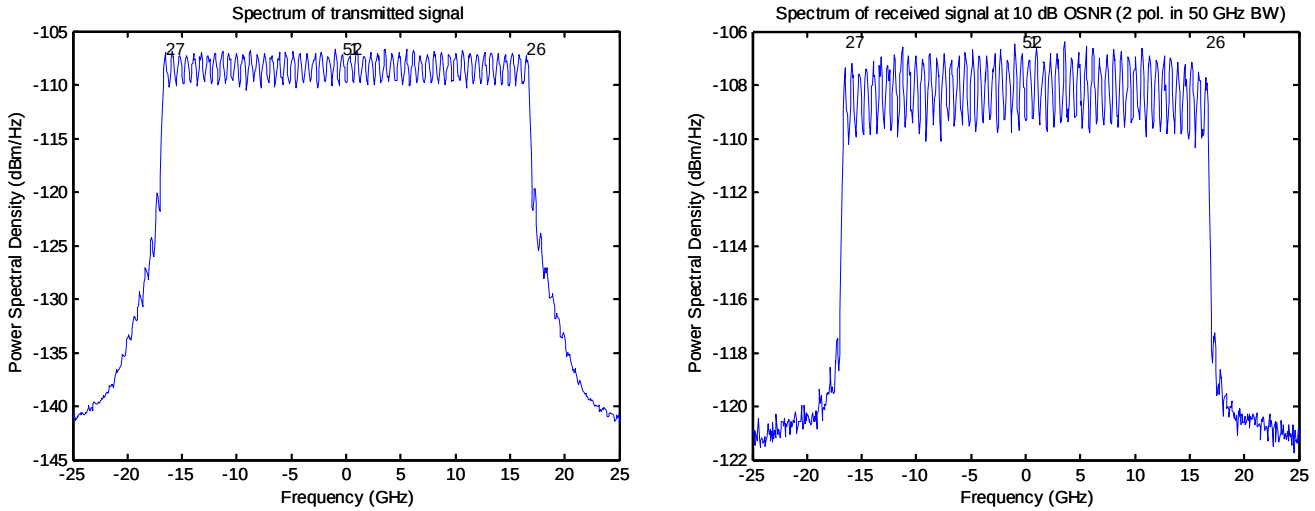


**Fig. 3.** Power spectra of transmitted and received OFDM signals, for $N_u$ = 52 used subcarriers. Note that subcarriers 1 and 52 are near the center, while subcarriers 26 and 27 are at the edges.

Fig. 4 shows signals at the inputs and outputs of the transmitter D/A converters. In Fig. 1, we see that prior to the D/A converters, the signals are hard-clipped to the range between $\pm CL$, and then mapped by a $\sin^{-1}()$ function to the range $\pm V_\pi$. We have used a value $V_\pi$ = 5 V so, in principle, these signals should cover the range between ±5 V. In this initial simulation example, the clipping level $CL$ has been chosen a little larger than necessary, so the signals never approach the clipping limits of $\pm CL$ or $\pm V_\pi$. In Fig. 4, the first column shows scatter plots of I vs. Q samples after clipping and $\sin^{-1}()$ predistortion, while the second column shows these after quantization (since we have used 8 bits here, quantization effects are not visible). The third and fourth columns show the quantized I and Q components at the D/A inputs and the modulator drive waveforms that the D/A converters interpolate from these. Close examination shows that the interpolated waveforms do not pass precisely through the D/A input samples, because the D/A converter is a non-ideal interpolator with a Butterworth response (as opposed to the ideal interpolator, which has an ideal lowpass response).

Fig. 5 shows the signals at the inputs and outputs of the receiver A/D converters. The first two columns show the waveforms of the I and Q components and the samples taken by the A/D converter. The third column shows scatter plots of I vs. Q samples before quantization. The fourth column shows scatter plots of the I vs. Q samples after they have been clipped to lie within the quantizer range of ±0.375 V and then quantized (since we have used 8 bits here, quantization effects are not visible).

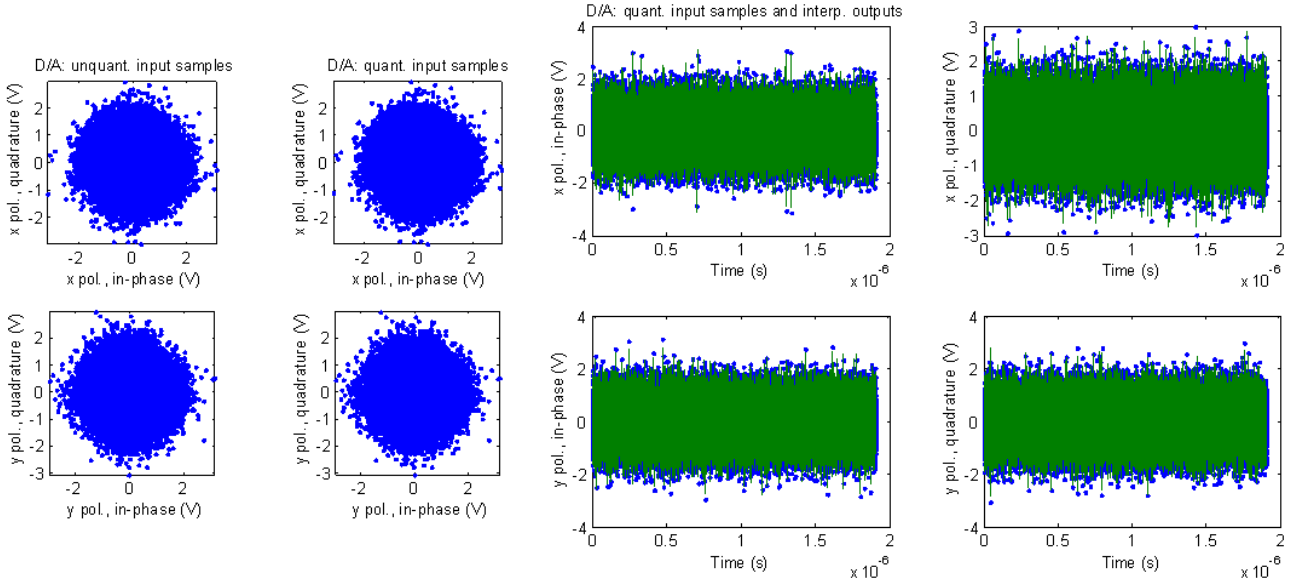


**Fig. 4.** D/A converters at OFDM transmitter. Left-hand figures show scatter plots of I and Q samples after clipping and nonlinear predistortion at D/A converter inputs, without quantization and including quantization. Right-hand figures show quantized samples at D/A converter inputs (blue dots) and waveforms at D/A converter outputs (green lines).

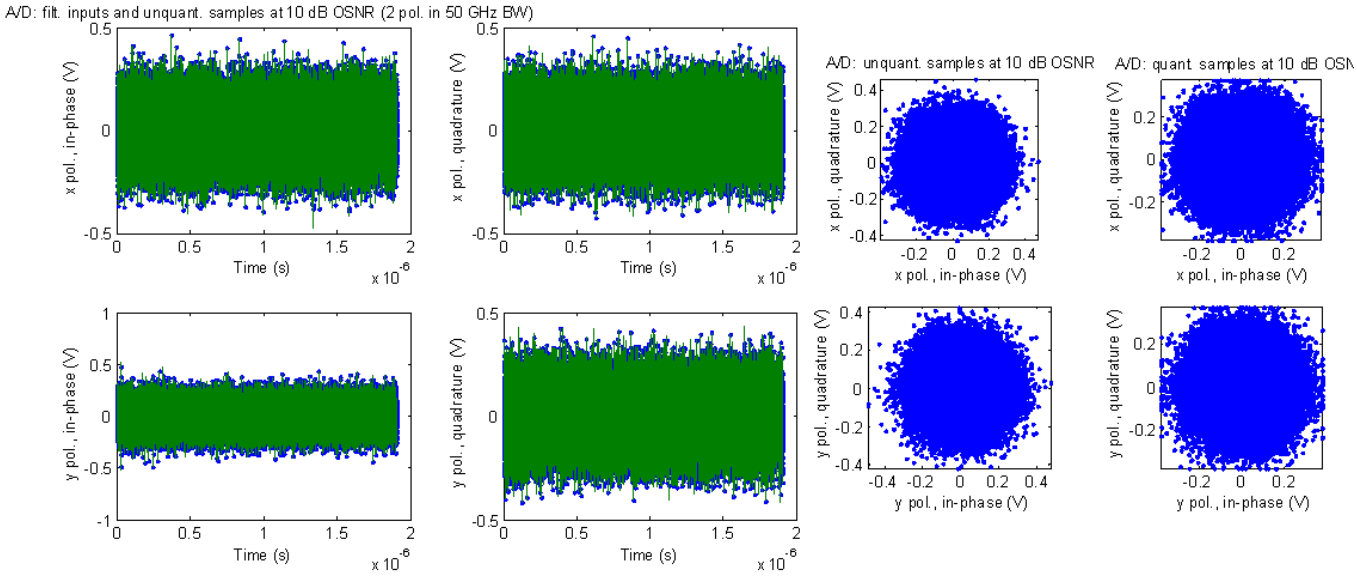


**Fig. 5.** A/D converters at OFDM receiver. Left-hand figures show waveforms at A/D converter inputs (green lines) and unquantized samples (blue dots). Right-hand figures show scatter plots of I and Q samples without quantization and including clipping and quantization.

Fig. 6 shows adaptation of the adaptive equalizer over the 1024 symbol periods simulated here (recall the symbol duration is $T_{ofdm} = N_u/R_s = 4N_u/R_b = 1.857$ ns). The top row shows the step size parameter, which starts with an initial value $\mu = 0.005$, and is then reduced by a factor of 10 after 768 symbol periods. It also shows that during the first 128 symbol intervals, a training sequence is sent, after which live data can be sent, and the equalizer can operate in decision-directed mode. In Fig. 6, the bottom row

shows the absolute squared error in the equalizer vs. symbol interval for four representative subcarriers (smoothed over 8 symbol intervals). The center subcarriers 1 and 52 adapt faster, and reach a lower squared error than the edge subcarriers 26 and 27, because optical filtering reduces the OSNR in the edge subcarriers.

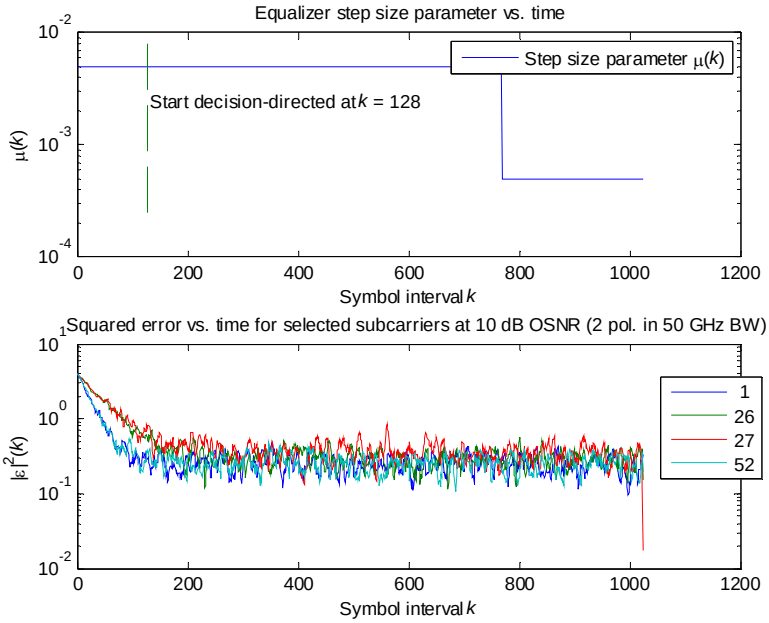


**Fig. 6.** Adaptive equalizer in OFDM receiver. Top plot shows LMS algorithm step size parameter vs. symbol interval. Bottom plot shows squared error vs. time for center subcarriers 1 and 52 and edge subcarriers 26 and 27.

Fig. 7 shows the magnitudes and phases of the coefficients in the receiver equalizers. It compares the ideal fixed equalizer (computed with perfect knowledge of the CD, PMD, optical filtering and receiver electrical filtering) to the adaptive equalizer. In the absence of PMD, the off-diagonal equalizer components (12 and 21) would be zero. Here, with PMD present, all four components are nonzero, and the magnitudes show significant variation over frequency. The phases of the equalizer are dominated by a quadratic frequency dependence, which compensates the CD. The magnitudes of the adaptive equalizer sometimes differ slightly from the ideal equalizer, but the phases of the adaptive equalizer consistently agree with the ideal equalizer (fortunately, only the phases are critical for detection of QPSK).

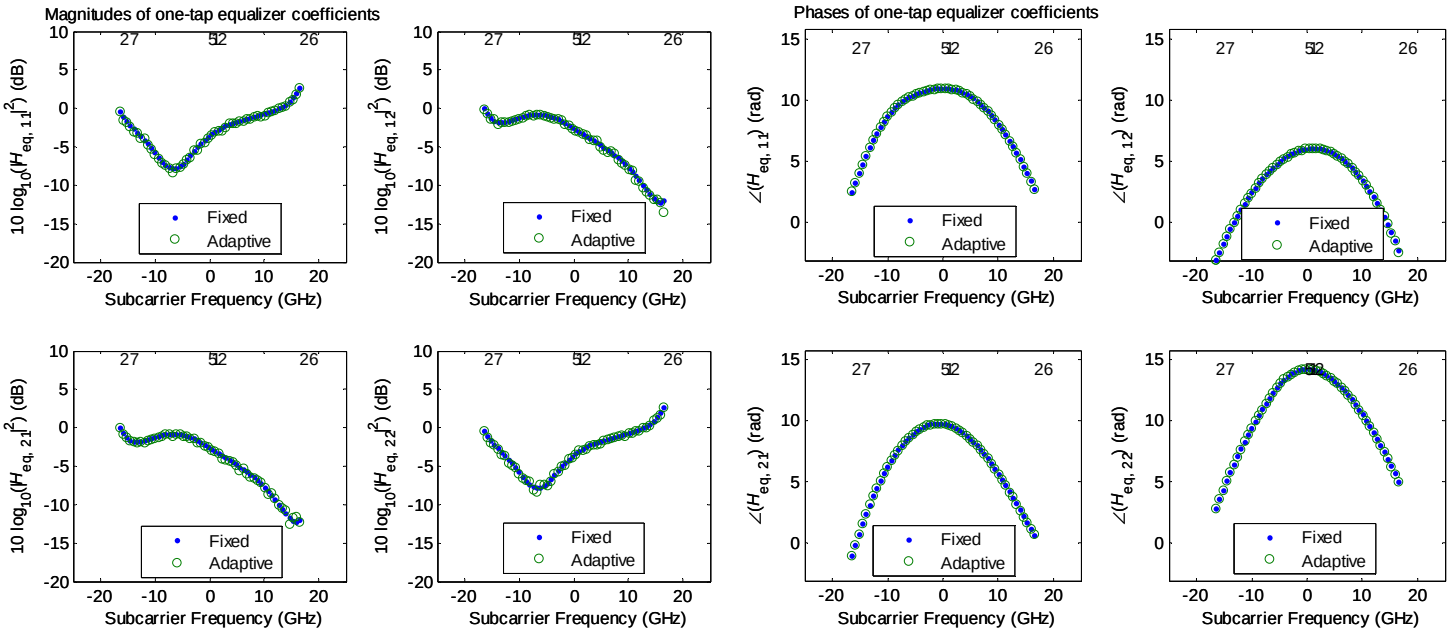


**Fig. 7.** Equalizer in OFDM receiver, showing ideal fixed equalizer (blue dots) and adaptive equalizer (green circles). The left plots show the magnitudes of equalizer coefficients vs. subcarrier frequency. The right plots show the phases of equalizer coefficients vs. subcarrier frequency.

Fig. 8 shows scatter plots of the constellation diagrams at the receiver equalizer outputs for four representative subcarriers. In each case, the ideal fixed equalizer is compared to the adaptive equalizer. Center subcarriers 1 and 52 exhibit slightly better constellation diagrams than edge subcarriers 26 and 27, because of optical filtering effects. In all cases, the adaptive equalizer gives results nearly indistinguishable from the ideal fixed equalizer.

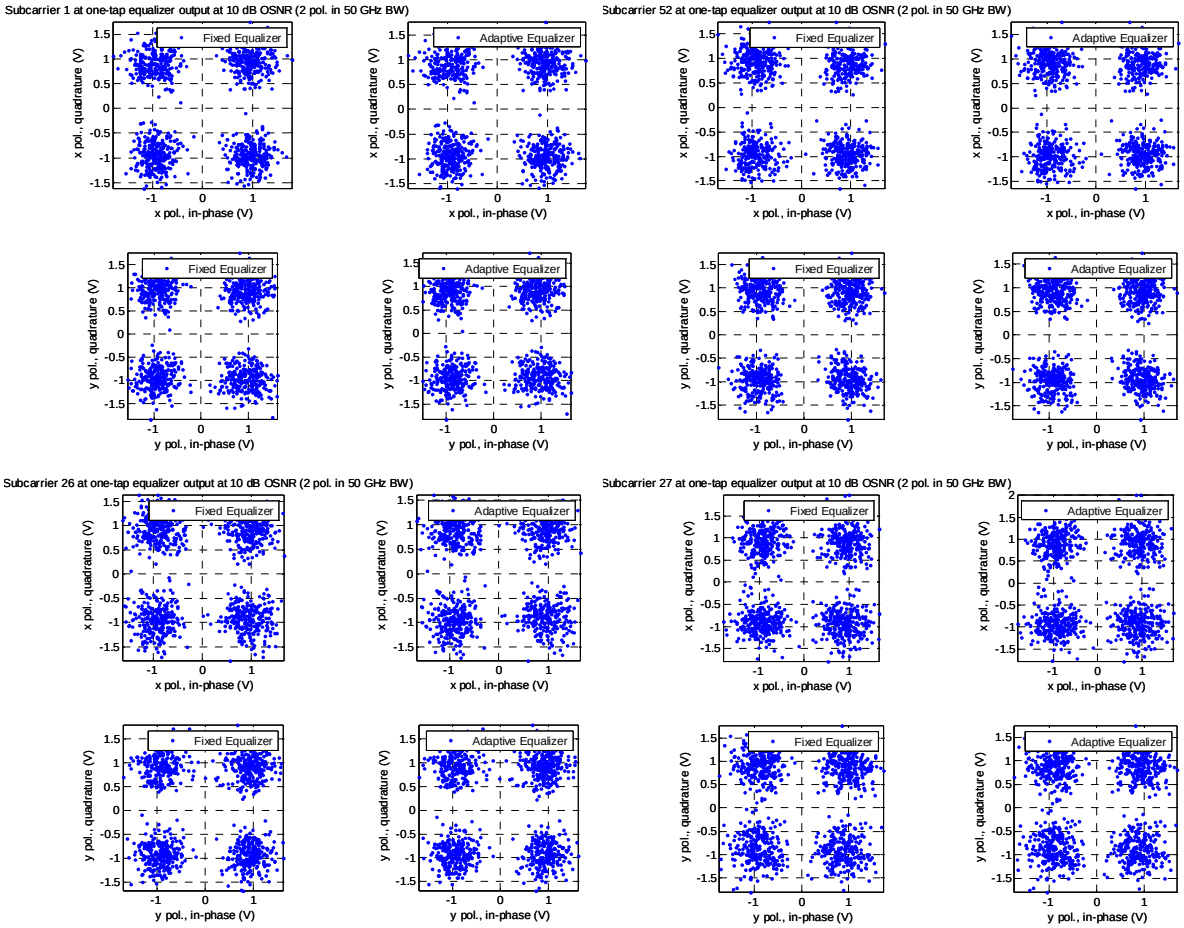


**Fig. 8.** Scatter plots of QPSK constellations in *x* and *y* polarizations at equalizer outputs for center subcarriers 1 and 52 and edge subcarriers 26 and 27. For each subcarrier, the first column shows an ideal fixed equalizer, and the second column shows an adaptive equalizer.

Fig. 9 shows the BER vs. transmitted power and BER vs. OSNR (this is the overall BER of the entire 112 Gbit/s bit stream). The ideal fixed equalizer and adaptive equalizer are compared, and are seen to give nearly identical results.

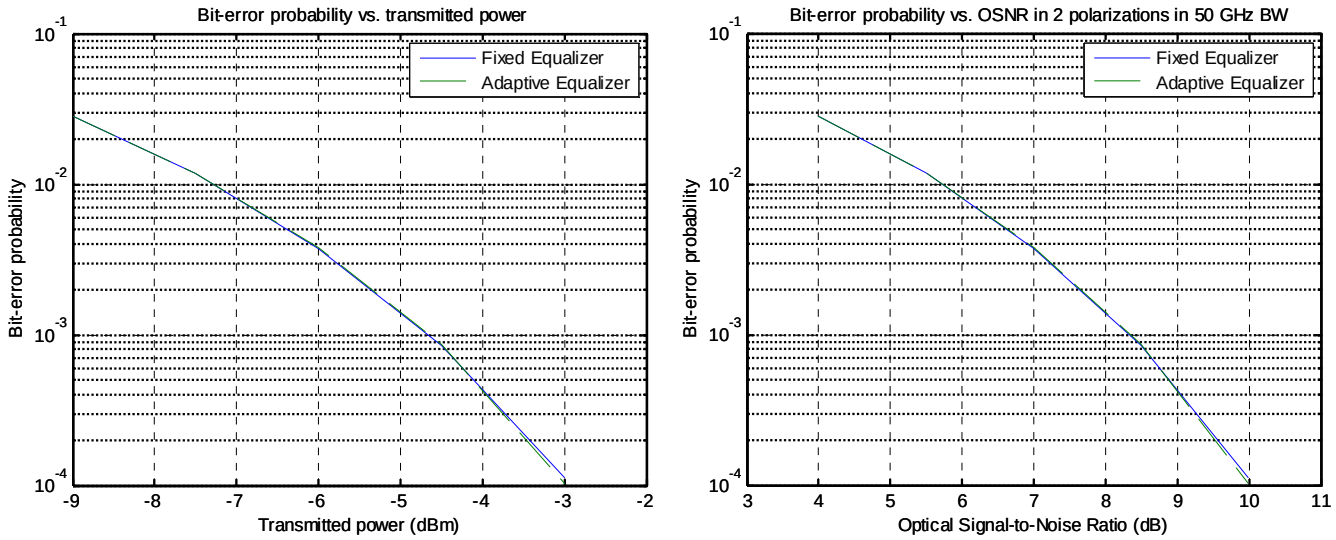


**Fig. 9.** Bit-error ratio performance of OFDM system. Left graph shows BER vs. transmitted power, while right graph shows BER vs. OSNR (in two polarizations in 50-GHz bandwidth). In each case, an ideal fixed equalizer (blue solid line) and adaptive equalizer (green dashed line) are compared.

### *4. System Performance with Unconstrained Transmitter and Receiver Complexity*

In this section, we adjust key OFDM parameters to determine the effect on system performance. Based on detailed analysis and simulations [2], we know that for the range of uncompensated CD considered here (around 1360 ps/nm), the choice $N_u$ = 52, $N_c$ = 64 is a good choice: (a) the cyclic prefix penalty $\left(N_c + N_{pre,os}\right)/N_c$ is small, (b) the oversampling ratio $N_c/N_u \approx 1.23$ is sufficiently large, (c) $N_c$ is an integer power of 2, and (d) the number of subcarriers is as small as possible. Hence, for simplicity, we will not vary $N_u$ or $N_c$, and will only vary the cyclic prefix length $N_{pre}$. Unless noted otherwise, we use all the same parameters as in the simulation example of Section 3(b) above. System performance is quantified in terms of the OSNR required to achieve $10^{-3}$ BER.

### *a. Optimization of Cyclic Prefix with No Dispersion*

Here, we assume no CD and no PMD, and an optical filter bandwidth of 50 GHz. Fig. 10 shows the OSNR requirement for $10^{-3}$ BER vs. cyclic prefix length $N_{pre}$. We see that a cyclic prefix length $N_{pre}$ = 1 or 2 is sufficient (the choice $N_{pre}$ = 0 does not work well, because of the temporal memory of the transmitter and receiver filters). The OSNR requirement for $10^{-3}$ BER is about 7.5 dB.

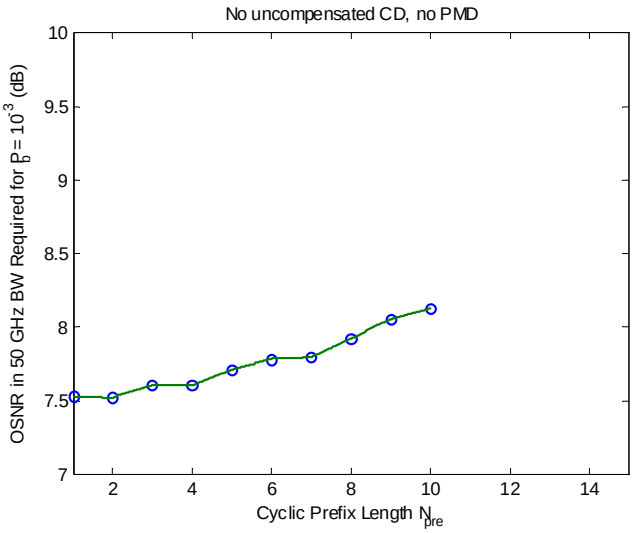


**Fig. 10.** Back-to-back system performance (in terms of OSNR required for $10^{-3}$ BER) as a function of cyclic prefix length $N_{pre}$. There is no CD and no PMD, and the optical filter bandwidth is 50 GHz.

### *b. Optimization of Cyclic Prefix for Chromatic Dispersion*

Here, we assume an uncompensated CD of 1360 ps/nm, no PMD, and an optical filter bandwidth of 50 GHz. Fig. 11 shows the OSNR requirement for $10^{-3}$ BER vs. cyclic prefix length $N_{pre}$. We see that a cyclic prefix length $N_{pre}$ = 10 is optimal (in agreement with [2]). This corresponds to an oversampled cyclic prefix length $N_{pre,os}$ = 13. When $N_{pre}$ << 10, the cyclic prefix is not long enough to insure orthogonality between different subcarriers, so ISI occurs. When $N_{pre}$ >> 10, transmission of the extra cyclic prefix samples increases the optical power (and sampling rate), while providing no benefit. At the optimal cyclic prefix $N_{pre}$ = 10, the OSNR requirement for $10^{-3}$ BER is 8.3 dB, about 0.8 dB higher than in the case without CD. If we compare the cyclic prefix penalty for $N_{pre}$ = 10 ($N_{pre,os}$ = 13) to that for $N_{pre}$ = 2 ($N_{pre,os}$ = 3), the increase in the penalty is given by $10 \cdot \log_{10}((52 + 13)/(52 + 3)) \approx 0.7$ dB, which accounts for nearly all of the increased OSNR requirement.

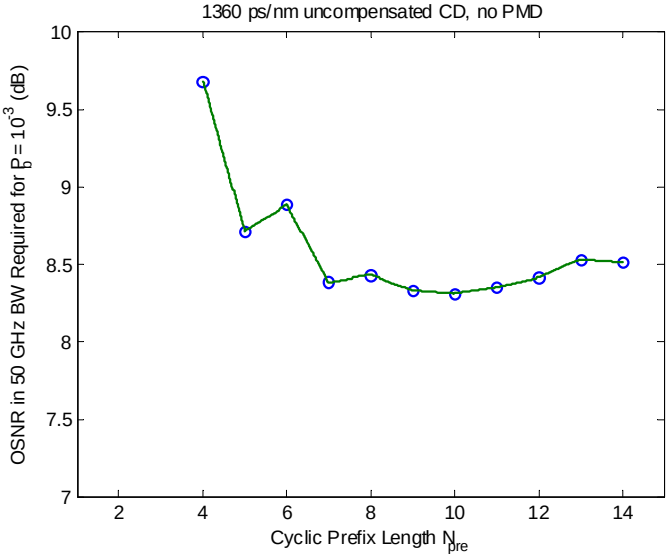


**Fig. 11.** System performance (in terms of OSNR required for $10^{-3}$ BER) for fixed CD as a function of cyclic prefix length $N_{pre}$. The uncompensated CD is 1360 ps/nm. There is no PMD, and the optical filter bandwidth is 50 GHz.

### *c. Impact of Chromatic Dispersion*

Here, we fix the cyclic prefix length at $N_{pre}$ = 10. We assume no PMD and an optical filter bandwidth of 50 GHz. We vary the uncompensated CD. Fig. 12 shows the OSNR requirement for $10^{-3}$ BER vs. uncompensated CD. The cyclic prefix has been optimized for CD of 1360 ps/nm, and above a CD of 1500 ps/nm, the penalty begins to rise steeply, because the cyclic prefix is no longer sufficient to maintain orthogonality between the different subcarriers.

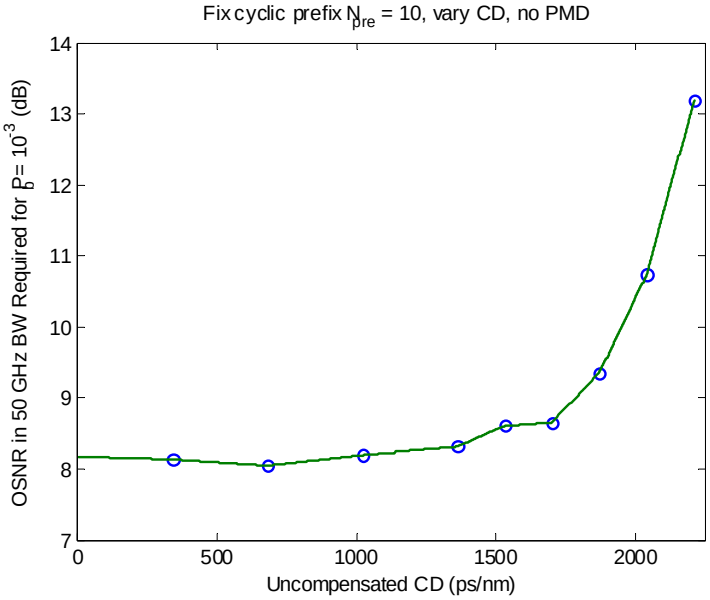


**Fig. 12.** System performance (in terms of OSNR required for $10^{-3}$ BER) for fixed cyclic prefix length $N_{pre}$ = 10 as a function of uncompensated CD. There is no PMD, and the optical filter bandwidth is 50 GHz.

### *d. Impact of Polarization-Mode Dispersion*

Here, we fix the cyclic prefix length at $N_{pre}$ = 10. We assume an uncompensated CD of 1360 ps/nm, and an optical filter bandwidth of 50 GHz. We introduce PMD and study its impact. Fig. 13 shows the frequency-dependent DGD magnitude and output SOP for three PMD realizations, each corresponding to a mean DGD of 50 ps. Fig. 14 shows the OSNR requirement for $10^{-3}$ BER vs. the mean DGD. We show three realizations for each value of the mean DGD. We also show three instances of no PMD (these are plotted at a mean DGD of zero). We observe that there is little or no degradation from PMD until the mean DGD reaches 50 ps. This is because until such high DGD values are reached, the temporal memory from PMD is much shorter than that from CD.

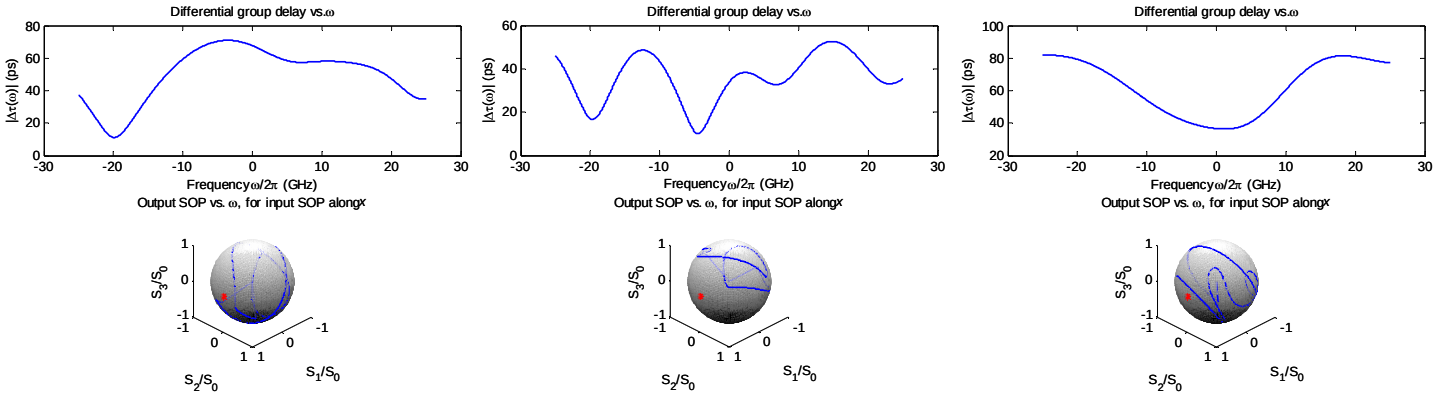


**Fig. 13.** Three realizations of PMD corresponding to 50-ps mean DGD. In each realization, the top graph shows magnitude of DGD as a function of frequency, while the bottom graph shows the output SOP as a function of frequency, for the input SOP along the *x* axis.

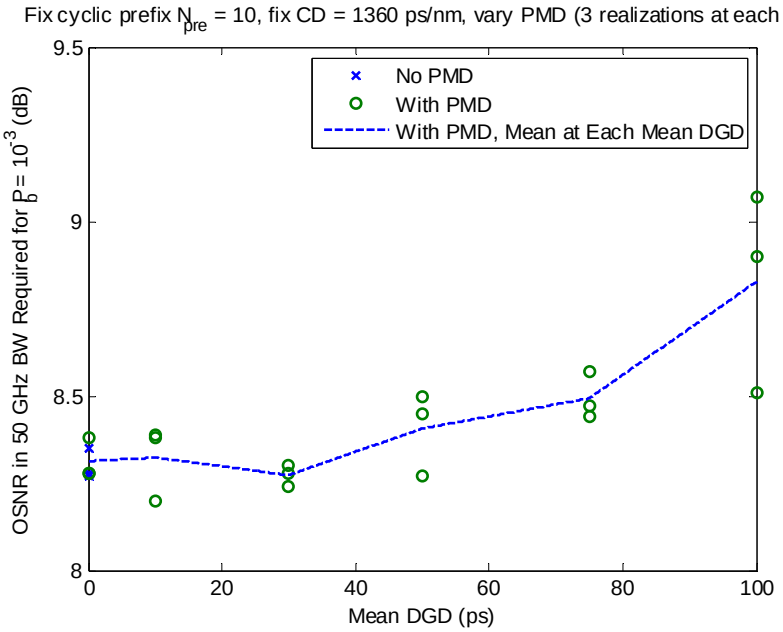


**Fig. 14.** System performance (in terms of OSNR required for $10^{-3}$ BER) for fixed cyclic prefix length $N_{pre}$ = 10 as a function of mean DGD. The uncompensated CD is 1360 ps/nm, and the optical bandpass filter bandwidth is 50 GHz. At each mean DGD, three realizations of the PMD are shown. The case of no PMD is also shown.

### *e. Impact of Tight Optical Filtering*

Here, we fix the cyclic prefix length at $N_{pre}$ = 10. We assume an uncompensated CD of 1360 ps/nm, one realization of PMD with mean DGD of 30 ps, and an optical filter bandwidth of 50 GHz. We study the impact of tight optical filtering. We model the effect of all the (de)multiplexers and ROADMs by a single 2nd-order super-Gaussian filter, and we assume that half of the ASE noise is added before the filter, while half is added after the filter. Fig. 15 compares received optical spectra when the filter bandwidth (at −3 dB) is 50 GHz and 27 GHz. In the latter case, the edge subcarriers are attenuated very significantly in comparison to the center subcarriers, and significant degradation would be expected. Fig. 16 shows the OSNR requirement for $10^{-3}$ BER vs. the optical filter bandwidth bandwidth (at −3 dB). When the filter bandwidth is reduced to 30 GHz, the OSNR penalty already exceeds 1 dB, and when it is reduced to 27

GHz, it exceeds 2 dB. In my previous studies of single-carrier PM-QPSK [5], at a bit rate of nearly 120 Gbit/s, I found that the optical filtering penalty at 27 GHz is about 1 dB, and the penalty at 25 GHz is about 1.6 dB. Thus, the simple OFDM scheme considered here is clearly more sensitive to tight optical filtering than is single-carrier modulation. It is possible to modify OFDM to make it more tolerant to tight optical filtering, but this would require increasing the modulation order beyond QPSK (e.g., to 8-QAM or 16-QAM) on some or all of the subcarriers.

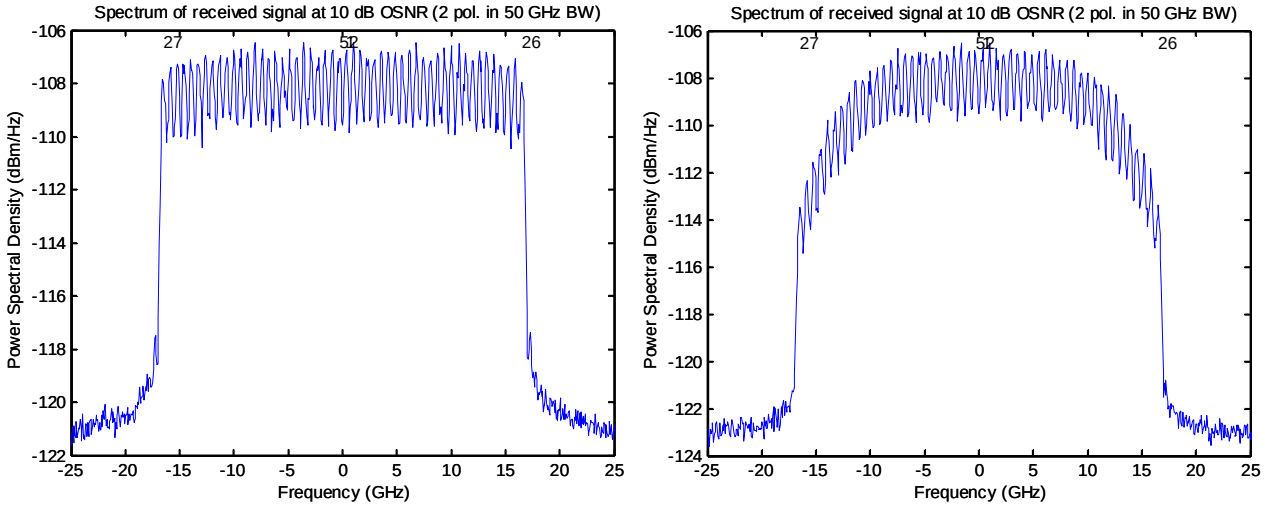


**Fig. 15.** Power spectra of received OFDM signals. Left graph: 50-GHz optical filter bandwidth. Right graph: 27-GHz optical filter bandwidth.

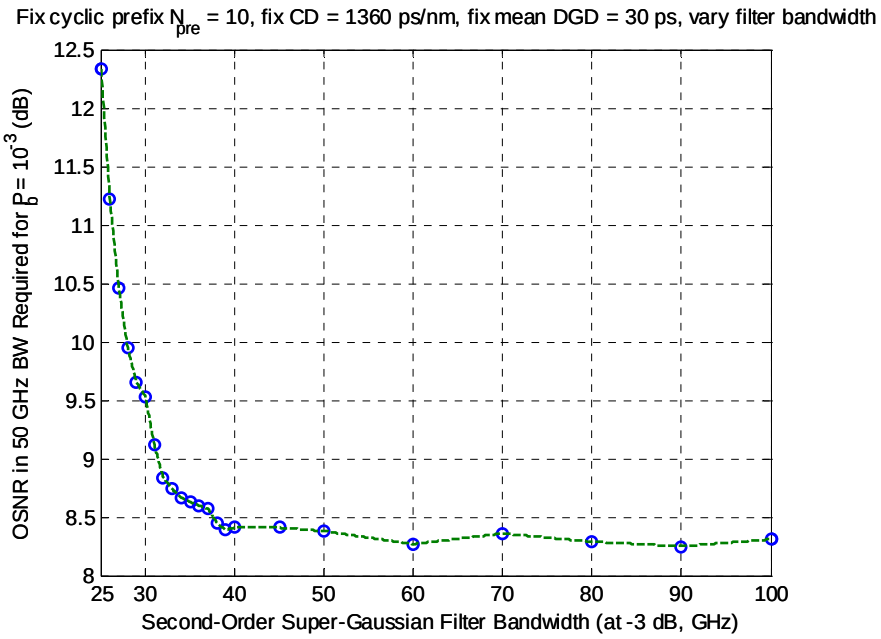


**Fig. 16.** System performance (in terms of OSNR required for $10^{-3}$ BER) as a function of bandwidth of second-order super-Gaussian optical bandpass filter. Half of the noise originates before the filter, and half originates after the filter. The cyclic prefix length is $N_{pre}$ = 10. The uncompensated CD is 1360 ps/nm, and the mean DGD is 30 ps.

### *5. Impact of Constrained Transmitter and Receiver Complexity*

In this section, we study the effect of transmitter and receiver complexity constraints on system performance. Unless noted otherwise, we use all the same parameters as in the simulation example of Section 3(b) above. In particular, we always consider $N_u$ = 52, $N_c$ = 64, $N_{pre}$ = 10. We always consider uncompensated CD of 1360 ps/nm, DGD of 30 ps, and an optical filter bandwidth of 50 GHz. System performance is quantified in terms of the OSNR required to achieve $10^{-3}$ BER.

#### *a. Impact of Transmitter Clipping and Quantization*

As explained in Section 2 above, the OFDM transmitter must be designed carefully to achieve good signal quality with a limited number of D/A quantization bits, while maintaining reasonably high optical power efficiency. As shown in Fig. 1, prior to the D/A converters, the signals are hard-clipped to the range between $\pm CL$, and then mapped by a $\sin^{-1}()$ function to the range $\pm V_\pi$. The optimal choice of clipping level $CL$ depends on the number of D/Q quantization bits (and on the number of subcarriers $N_c$, the cyclic prefix length $N_{pre}$, and the target BER). When the clipping level is too small, clipping causes excessive noise; when the clipping level is too high, quantization noise becomes excessive.

We define the transmitter optical power efficiency as the ratio between the average optical power of the PM-OFDM signal and the CW optical power of the laser, $P_{mod}/P_{laser}$, ignoring any loss in the modulators or in the polarization-multiplexing components. Note that for single-carrier PM-QPSK using NRZ pulses, the transmitter optical power efficiency should be close to unity (0 dB). In the top portion of Fig. 17, we show the transmitter optical power efficiency $10\cdot\log_{10}(P_{mod}/P_{laser})$ as a function of the clipping level $CL$. We see that the efficiency increases as we decrease the clipping level, as expected. In the useful range of clipping levels, between 0.4 V and 0.25 V, the transmitter efficiency varies from about −11 dB to about −7 dB. By contrast, for single-carrier PM-QPSK using NRZ pulses, the transmitter optical power efficiency should be much closer to 0 dB.

In the bottom portion of Fig. 17, we show the OSNR requirement for $10^{-3}$ BER vs. clipping level for different number of transmitter D/A quantization bits between 4 and 8 bits. For 8-bit quantization, the optimal clipping level is $CL$ = 0.4 V, and the OSNR requirement is about 8.3 dB. For 5-bit quantization, the optimal clipping level is $CL$ = 0.25 V, and the OSNR requirement is about 8.7 dB, a penalty of about 0.4 dB.

Fig. 18 shows scatter plots of the I vs. Q samples at the D/A converter inputs for these two cases, after clipping but before quantization, and after both clipping and quantization. With 5-bit quantization, the optimal clipping level corresponds to a significant degree of clipping. We have used a value $V_\pi$ = 5 V, and we see that with optimized choice of the clipping level, the signals do cover the entire range between ±5 V.

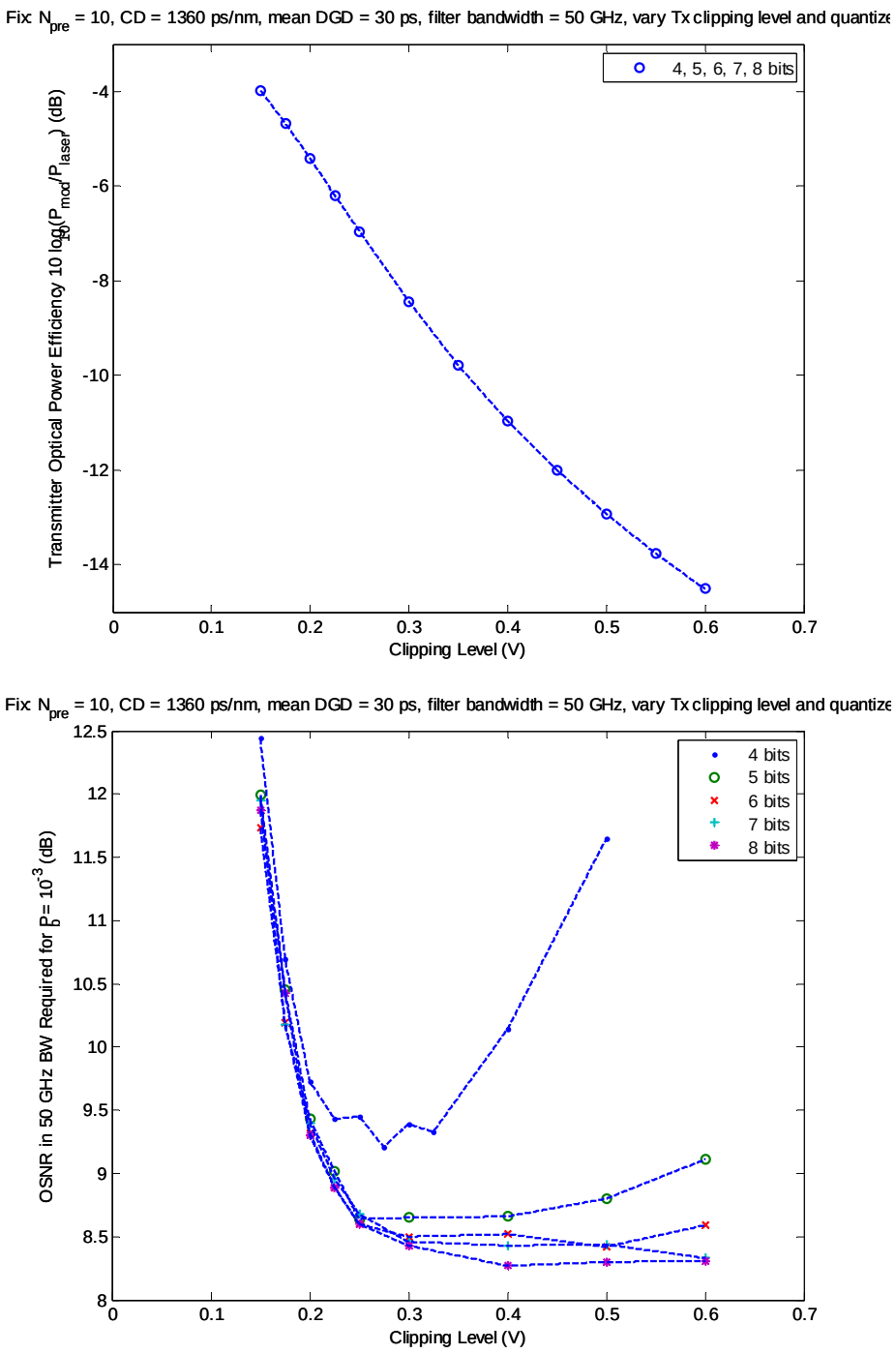


**Fig. 17.** Top graph: transmitter optical power efficiency as a function of transmitter clipping level. Bottom graph: system performance (in terms of OSNR required for $10^{-3}$ BER) as a function of transmitter clipping level and number of D/A quantization bits. The cyclic prefix length is $N_{pre}$ = 10. The uncompensated CD is 1360 ps/nm, the mean DGD is 30 ps, and the optical filter bandwidth is 50 GHz.

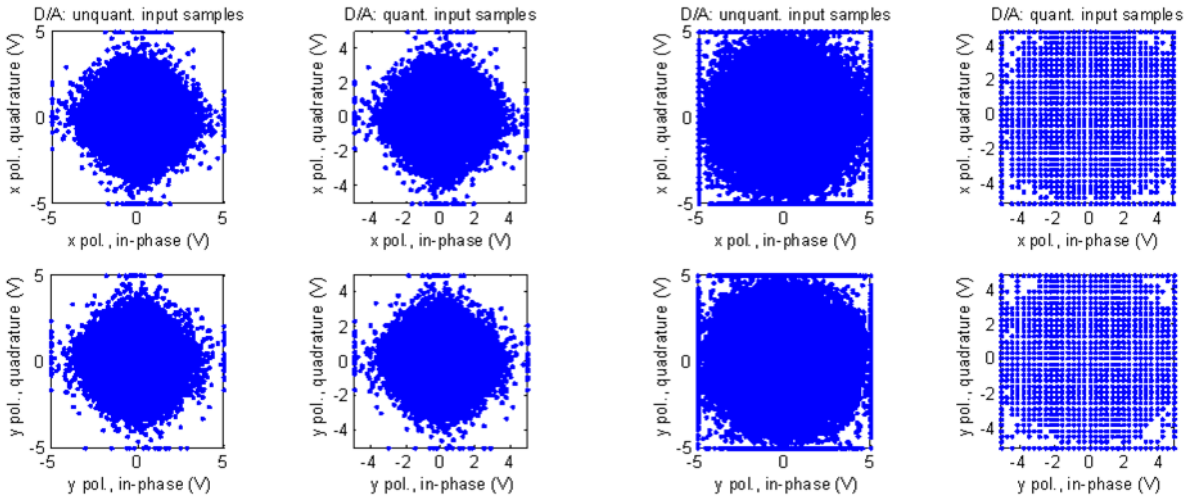


**Fig. 18.** D/A converters at OFDM transmitter, showing scatter plots of I and Q samples after clipping and nonlinear predistortion at D/A converter inputs, without quantization and including quantization. The left figure considers a 0.4-V clipping level and 8-bit quantization. The right figure considers a 0.25-V clipping level and 5-bit quantization.

### *b. Impact of Receiver Clipping and Quantization*

Here, we study the effect of clipping and quantization at the receiver A/D converter. Unlike the case of the transmitter D/A, here we define a quantizer range that is the full range between the positive and negative clipping levels. For a given number of quantization bits, there is an optimal quantizer range. When the quantizer range is too small, there will be excessive noise from clipping, while when the quantizer range is too large, there will be excessive noise from quantization. The optimal quantizer range depends on several parameters, including the number of subcarriers $N_c$, the cyclic prefix length $N_{pre}$, and the target BER.

In Fig. 19, we show the OSNR requirement for $10^{-3}$ BER vs. quantizer range for different number of receiver A/D quantization bits between 4 and 8 bits. For 8-bit quantization, the optimal quantizer range is about 0.7 V, and the OSNR requirement is about 8.25 dB. For 5-bit quantization, the optimal quantizer range is about 0.6 V, and the OSNR requirement is about 8.45 dB, a penalty of about 0.2 dB.

Fig. 20 shows scatter plots of the I vs. Q samples at the A/D converter inputs for these two cases, with neither clipping nor quantization, and with both clipping and quantization. With 5-bit quantization, the optimized quantizer range corresponds to a significant probability of clipping.

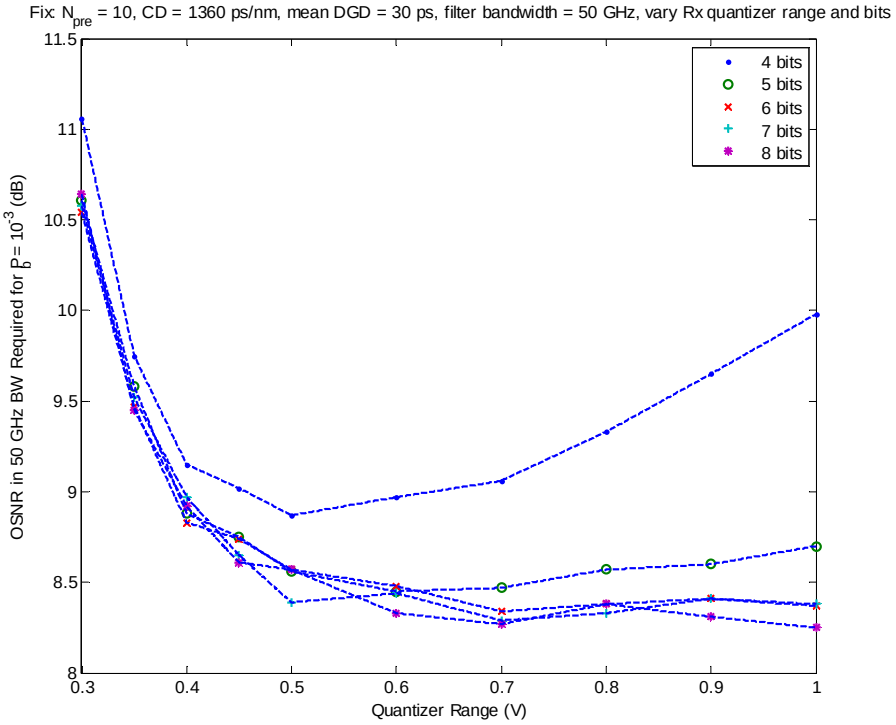


**Fig. 19.** System performance (in terms of OSNR required for $10^{-3}$ BER) as a function of receiver A/D quantizer range and number of quantization bits. The cyclic prefix length is $N_{pre}$ = 10. The uncompensated CD is 1360 ps/nm, the mean DGD is 30 ps, and the optical filter bandwidth is 50 GHz.

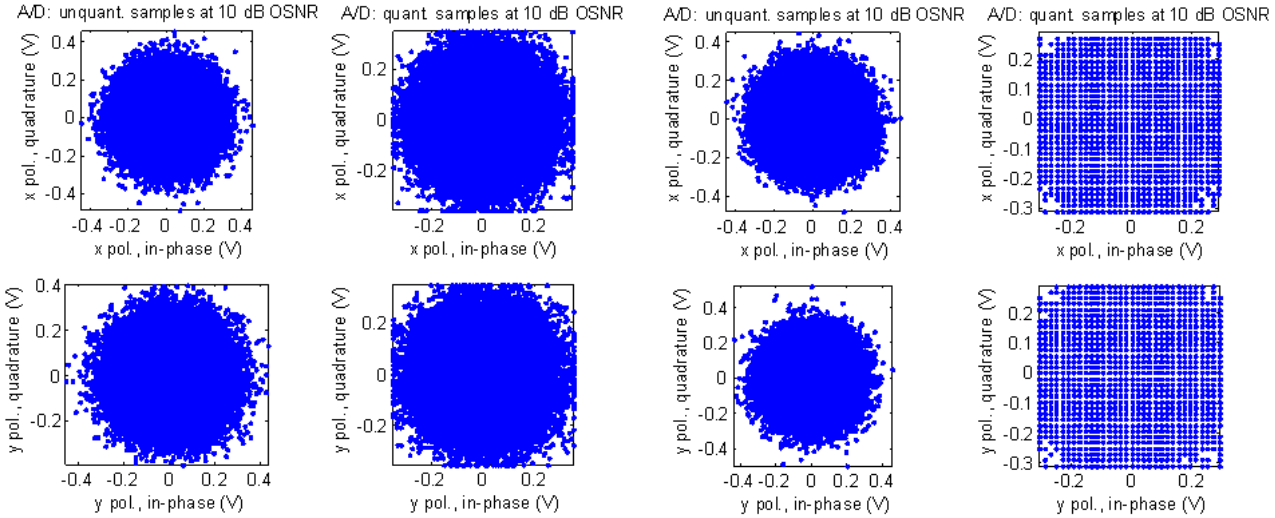


**Fig. 20.** A/D converters at OFDM receiver, showing show scatter plots of I and Q samples without clipping/quantization and including clipping/quantization. The left figure considers a 0.7-V quantizer range and 8-bit quantization. The right figure considers a 0.6-V quantizer range and 5-bit quantization.

***References***


1. E. Ip, A. P. T. Lau, D. J. F. Barros and J. M. Kahn, "Coherent Detection in Optical Fiber Systems", *Optics Express*, vol. 16, no. 2, pp. 753-791, January 21, 2008.
2. D. J. F. Barros and J. M. Kahn, "Optimized Dispersion Compensation Using Orthogonal Frequency-Division Multiplexing", to be published in *J. of Lightwave Technol.*
3. D. J. F. Barros and J. M. Kahn, "Optical Modulator Optimization for Orthogonal Frequency-Division Multiplexing", subm. to *J. of Lightwave Technol.*, June 2008.
4. A. J. Lowery, "Fiber Nonlinearity Mitigation in Optical Links That Use OFDM for Dispersion Compensation", *Photon. Technol. Lett.*, vol.19, no.19, pp.1556-1558, Oct.1, 2007. This author has published several very closely related papers in *Optics Express* and other journals.
5. J. M. Kahn, "100 Gbit/s PM-QPSK NRZ Simulations", technical report submitted to StrataLight Communications, November 26, 2007.